(200)
TEQ7r

Geology and Mineralogy

This document consists of 36 pages.
Series A.

UNITED STATES DEPARTMENT OF THE INTERIOR

GEOLOGICAL SURVEY

THE CRYSTAL STRUCTURE OF POTASSIUM METAVANADATE, MONOHYDRATE, $KVO_3 \cdot H_2O$*

By

C. L. Christ, Joan R. Clark, and H. T. Evans, Jr.

U.S. GEOLOGICAL SURVEY
DENVER
JUN 7 1983
LIBRARY
GEOLOGIC DIVISION

February 1954

Trace Elements Investigations Report 406

This preliminary report is distributed without editorial and technical review for conformity with official standards and nomenclature. It is not for public inspection or quotation.

*This report concerns work done on behalf of the Division of Raw Materials of the U. S. Atomic Energy Commission.

USGS - TEI-406

GEOLOGY AND MINERALOGY

Distribution (Series A)	No. of copies
American Cyanamid Company, Winchester	1
Argonne National Laboratory	1
Atomic Energy Commission, Washington	2
Battelle Memorial Institute, Columbus	1
Carbide and Carbon Chemicals Company, Y-12 Area	1
Division of Raw Materials, Albuquerque	1
Division of Raw Materials, Butte	1
Division of Raw Materials, Denver	1
Division of Raw Materials, Douglas	1
Division of Raw Materials, Grants	1
Division of Raw Materials, Hot Springs	1
Division of Raw Materials, Ishpeming	1
Division of Raw Materials, New York	6
Division of Raw Materials, Phoenix	1
Division of Raw Materials, Richfield	1
Division of Raw Materials, Salt Lake City	1
Division of Raw Materials, Washington	3
Division of Research, Washington	1
Dow Chemical Company, Pittsburg	1
Exploration Division, Grand Junction Operations Office	1
Grand Junction Operations Office	1
Technical Information Service, Oak Ridge	6
Tennessee Valley Authority, Wilson Dam	1
U. S. Geological Survey:	
Alaskan Geology Branch, Washington	1
Fuels Branch, Washington	1
Geochemistry and Petrology Branch, Washington	15
Geophysics Branch, Washington	1
Mineral Deposits Branch, Washington	1
E. H. Bailey, Menlo Park	1
K. L. Buck, Denver	1
J. R. Cooper, Denver	1
N. M. Denson, Denver	1
C. E. Dutton, Madison	1
R. P. Fischer, Grand Junction	1
L. S. Gardner, Albuquerque	1
M. R. Klepper, Washington	1
A. H. Koschmann, Denver	1
R. A. Laurence, Knoxville	1
D. M. Lemmon, Washington	1
J. D. Love, Laramie	1
R. G. Petersen, Plant City	1
R. J. Roberts, Salt Lake City	1
Q. D. Singewald, Beltsville	1
J. F. Smith, Jr., Denver	1
R. W. Swanson, Spokane	1
A. E. Weissenborn, Spokane	1
W. P. Williams, Joplin	1
TEPCO, Denver	2
TEPCO, RPS, Washington	2
(Including master)	78

CONTENTS

ILLUSTRATIONS

TABLES

THE CRYSTAL STRUCTURE OF POTASSIUM METAVANADATE MONOHYDRATE, $KVO_3 \cdot H_2O$

By C. L. Christ, Joan R. Clark, and H. T. Evans, Jr.

ABSTRACT

$KVO_3 \cdot H_2O$ is orthorhombic, Pnam, $a = 8.15_1$ A, $b = 13.58_6$, $c = 3.69_7$, $Z = 4$. A trial structure, established by the use of a vector shift method applied to the Patterson projection on (001), was refined by electron density projections including bounded projections, and by least squares analysis. In the structure each vanadium atom is linked to five oxygen atoms to form a distorted trigonal dipyramid; the polyhedra so formed share edges to form continuous chains parallel to the c axis. This fivefold coordination is analogous to that which exists in V_2O_5.

INTRODUCTION

When vanadium pentoxide is dissolved in a solution of potassium hydroxide, and the solution maintained at a pH between 6.5 and 8, clear colorless needles of both potassium metavanadate, KVO_3, and its monohydrate, $KVO_3 \cdot H_2O$, are readily produced on concentration and cooling. This pH range comprises the so-called "metavanadate" stability range, in contrast to the range of pH >10 corresponding to the "orthovanadates", the range from pH 8 to 10 corresponding to the "pyrovanadates", and the range corresponding to the orange "polyvanadates" from pH 6.5 to the isoelectric point at pH 1.6 at which point brown V_2O_5 hydrates precipitate. The system Na_2O-V_2O_5-H_2O, which is characterized in a general way

by the stability ranges referred to, has been the subject of considerable study of various workers and by various physical chemical methods. [See for example Düllberg (1903), Jander and Jahr (1933), Souchay and Carpeni (1946), Ducret (1951).] Although the reactions involved are usually considered to be a series of successive condensations toward higher molecular weight complexes with increasing acidity, no details have been established to date concerning any of the molecular structures, or any of the mechanisms involved. In the U. S. Geological Survey laboratories, we are making an attempt to approach the problem of the constitution and interrelation of the many phases present in the system K_2O-V_2O_5-H_2O by means of crystal structure analysis of the solids which appear. In this paper the crystal structure of $KVO_3 \cdot H_2O$ is described in detail. [A preliminary account has been given in Christ, Clark, and Evans (1953).] A study of the structure of KVO_3 has been completed and will be described in a forthcoming article.

KVO_3 and $KVO_3 \cdot H_2O$, although their crystal structures have been revealed to be entirely different, are very similar in chemical and physical properties and mode of genesis. Both are sparingly soluble in cold water and readily soluble in hot water and both have pronounced fibrous cleavage. When a potassium metavanadate solution is rapidly cooled, a crystalline precipitate characterized by fine hairlike needles appears, which is mainly KVO_3. As cooling slows at lower temperatures, needles of similar habit of $KVO_3 \cdot H_2O$ are also formed. On very slow crystallization by evaporation, radiating groups of blunt rods of $KVO_3 \cdot H_2O$ are produced, sometimes simultaneously and in contact with stubby, pseudo-octahedral crystals of KVO_3. $KVO_3 \cdot H_2O$ apparently converts to KVO_3 on grinding.

$KVO_3 \cdot H_2O$ was first recognized by Norblad (1875) and was noted by Fock (1889), but otherwise to our knowledge is not mentioned in the literature.

EXPERIMENTAL WORK

Preparation of crystals and chemical analysis

At the beginning of this investigation it was believed that the two compounds crystallizing in the pH range between 6.5 and 8 were polymorphic forms of KVO_3. The structure analysis, however, soon showed clearly that the substance dealt with here was a monohydrate and was entirely consistent with a compound of formula $KVO_3 \cdot H_2O$. With this in mind it was then possible to resolve the difficulties in chemical analysis which arose from the fact that mixtures were being dealt with. By very slow crystallization, mixtures were prepared containing crystals sufficiently large to ensure efficient separation. An analysis, in percent, of the $KVO_3 \cdot H_2O$ obtained in this way is given below:

	K_2O	V_2O_5	H_2O	Total
Found:	30.24	58.40	11.64	100.28
Theoretical:	30.18	58.28	11.54	100.00

Analyst, George B. Magin, Jr., U. S. Geological Survey

A drawing of the typical blunt-rod habit of $KVO_3 \cdot H_2O$ is given in figure 1.

Space group and unit cell dimensions

Zero and upper level photographs around [001], made on both Weissenberg and precession cameras and with both zirconium-filtered MoKα(Mo/Zr) and nickel-filtered CuKα(Cu/Ni) radiations, were used to

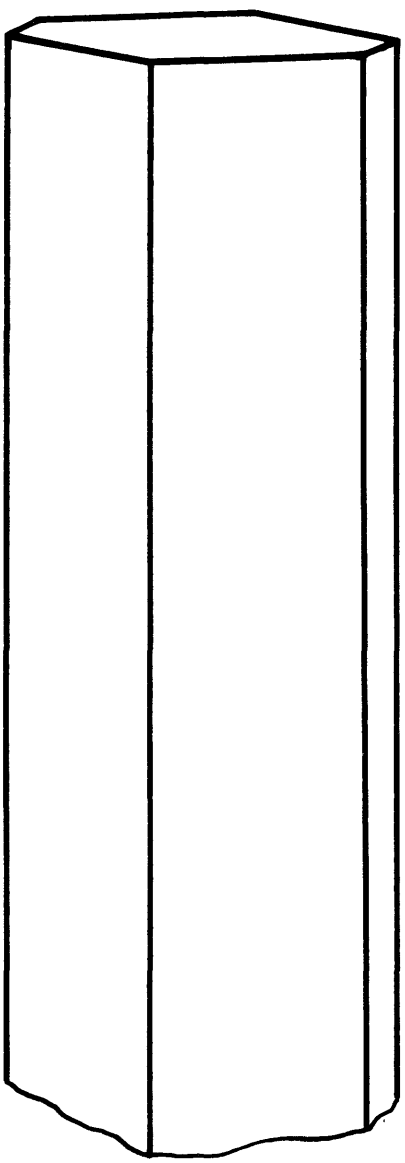

Figure 1.--Typical blunt-rod crystal of $KVO_3 \cdot H_2O$

establish the lattice type and symmetry. Systematic extinctions were found to be of the type $h0\ell$, $h \neq 2n$ and $0k\ell$, $k + \ell \neq 2n$. These lead to the space groups Pnam (D_{2h}^{16}) or Pna ($C_{2v}9$). Visual examination of the reflections obtained on rotation patterns made around [001] establishes that corresponding reflections on all even layer lines are similar, as are those on all odd layer lines. It follows that in this structure most atoms are situated on planes parallel to (001) and c/2 apart. This fact suggests that all the atoms lie on mirror planes in the space group Pnam, and on this assumption a satisfactory structure has been determined.

Lattice constant measurements were made with a precession camera, the crystal to film distance of which had been accurately calibrated by use of a quartz crystal. Patterns of the ($h0\ell$) and ($0k\ell$) zones were prepared using Mo/Zr radiation and were corrected for horizontal and vertical shrinkage. The values of the cell edges derived from these patterns were checked against those derived from a powder pattern made with Cu/Ni radiation. The powder data are given in table 1. As $KVO_3 \cdot H_2O$ converts to KVO_3 on grinding, it was impossible to prepare a powder pattern of $KVO_3 \cdot H_2O$ only; the data of table 1 correspond to the mixture. The crystallographic data for $KVO_3 \cdot H_2O$ are collected below:

Orthorhombic: Space group Pnam (D_{2h}^{16})

$a = 8.15_1 \pm 0.008$ A	cell contents $4(KVO_3 \cdot H_2O)$
$b = 13.58_6 \pm 0.010$	density (calc.) = 2.53 g cm^{-3}
$c = 3.69_7 \pm 0.004$	density (obs.) = 2.52 g cm^{-3}

(Moλ: Kα = 0.71069 A, Kα_1 = 0.70926 A)

Intensity measurements

For the intensity measurements multiple film Weissenberg patterns using Mo/Zr radiation were prepared. Three films interleaved with 0.0005 inch Ni foil were used for each exposure. The (hk0) and (hk1) zones were recorded from a prismatic crystal having nearly equidimensional cross section, approximately 0.1 x 0.1 mm. A comparison strip of intensities was prepared by recording a given reflection from the crystal for varying known lengths of time, using the same experimental set-up and crystal as was used in preparing the Weissenberg patterns. The estimated intensities were converted to $|F_{hk\ell}|^2$ values through the use of the Lorentz and polarization factor tables of Buerger and Klein (1945) for the hk0's and the Lp chart of Cochran (1948) for the hk1's. No attempt was made to correct for absorption effects, which were assumed to be relatively small owing to the small cross-sectional size of the crystal used and to use of MoKα radiation.

Other considerations

In the initial stages of the analysis the observed and calculated structure factors were related by use of the scaling constant k, where $k\Sigma|F_o| = \Sigma|F_c|$. Subsequently, the relationship $k|F_o| = |F_c| \exp\left[-B(\sin^2\theta)/\lambda^2\right]$ was used to fix the absolute scale of the observed structure factors, and the value of the coefficient B of the temperature factor. For the final values of the coordinates, B = 1.22 A^2 for the (hk0) zone and 0.71A^2 for the (hk1) zone.

The Hartree atomic scattering curve for $O^=$ was used for the oxygen atoms and for the water molecule. For K^+ a scattering curve corresponding

to the Thomas-Fermi values for K for $(\sin\theta)/\lambda \geq 0.1$ A^{-1}, and smoothed in to f = 18 for $(\sin\theta)/\lambda$ = 0 A^{-1}, was used. At the beginning of the structural analysis a curve prepared in an analogous fashion for V^{+5} was used. It was later found that significant improvement in the agreement between calculated and observed structure factors at small $(\sin\theta)/\lambda$ values was obtained when the Thomas-Fermi values for V were used. The subsequent refinement was made using these values. All values of the scattering factors were taken from the International Tables (1935).

Maxima on the electron density maps used in determining the structure were located by the method of Booth (1948).

DETERMINATION AND REFINEMENT OF THE STRUCTURE

The structural problem consists of determining the parameters of 1 potassium, 3 oxygen, and 1 water in the positions 4(c) of the space-group Pnam (International Tables, 1935). The relatively short c axis suggested the use of the Patterson projection on (001) for the determination of the essential features of this structure, and accordingly this projection was prepared with the $|F_{hk0}|^2$ values on an arbitrary basis and the $|F_{000}|^2$ term omitted. Buerger (1951) has shown how the Patterson projection on (001) for a crystal of similar symmetry and dimensions, berthierite $FeSb_2S_4$ (Pnam, a = 11.44, b = 14.12, c = 3.76 A, Z = 4), may be converted to an approximate electron density map through the use of his minimum function analysis. Buerger's procedure for $FeSb_2S_4$ was followed for $KVO_3 \cdot H_2O$ and the approximate $\rho_z(x,y)$ map shown in figure 2 was obtained.1/ From this map x and y coordinates for the two heavy

1/ It should be pointed out that with the F_{000}^2 term omitted it was necessary to contour all the levels of the Patterson map, including the negative ones, in order to finish with a meaningful approximate $\rho_z(x,y)$ map.

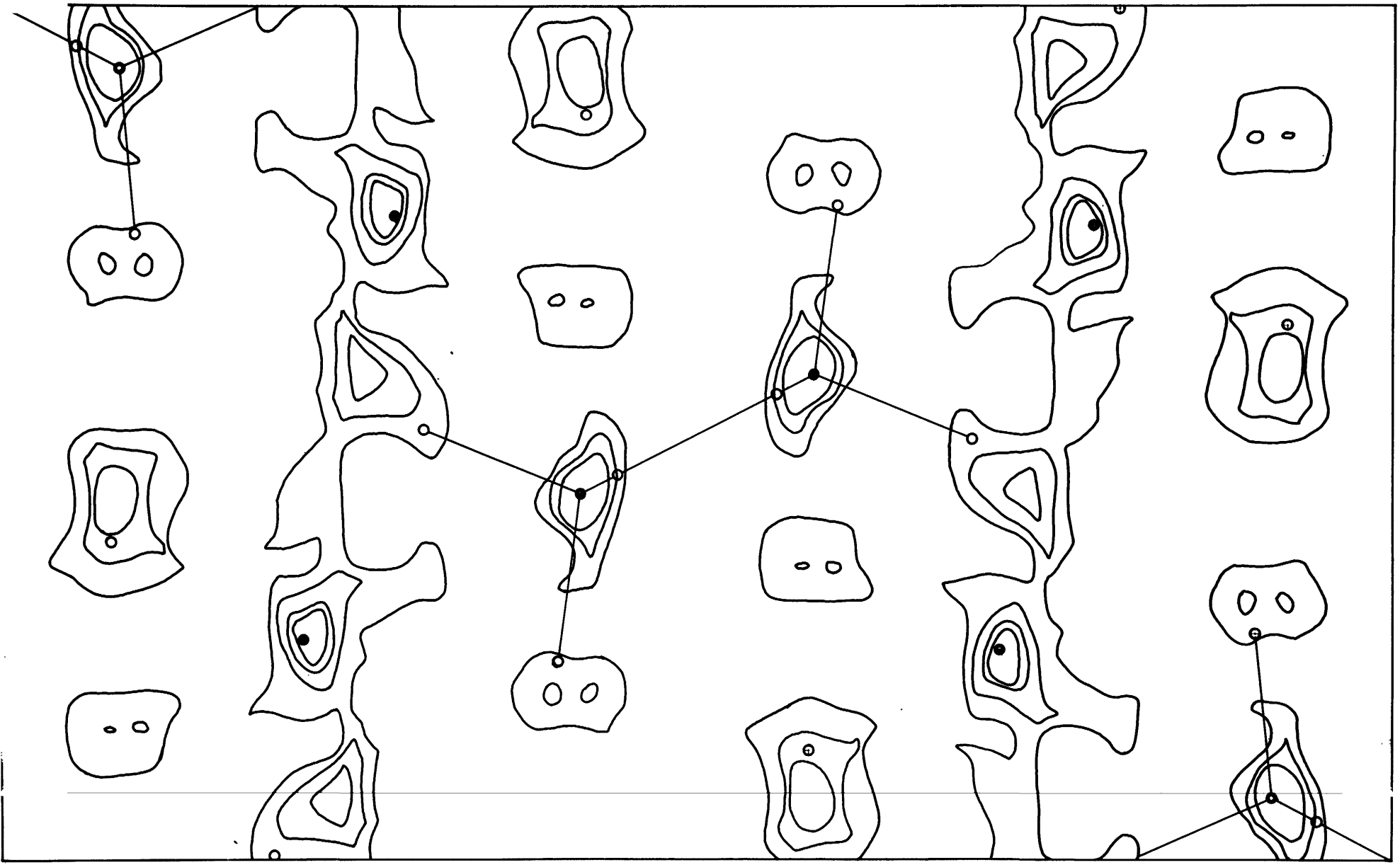

Figure 2.--Approximate $\rho_z(x,y)$ map obtained by the minimum function method (a axis vertical, b horizontal). The final atomic positions are indicated by the small circles.

atoms K and V were assigned and structure factors F_{hk0} calculated using the same atomic scattering curve for both atoms, that of K^+. These coordinates are given in column 1 of table 2, which lists the coordinates and discrepancy factor R found for each stage of the refinement. Signs calculated on the basis of these coordinates permitted the evaluation of $\rho_z(x,y)$ using 87 terms. From this map coordinates for all the atoms, but not for the water molecule, were assigned and a second $\rho_z(x,y)$ containing 136 terms calculated. Actually, a peak corresponding to the water molecule appeared on the first $\rho_z(x,y)$ map as well as on the approximate $\rho_z(x,y)$ map derived from the Patterson function. As it was believed that the compound was anhydrous, this peak was dismissed as being spurious, and was expected to disappear in subsequent electron density refinement, but at the completion of the second $\rho_z(x,y)$ map, it was realized that the peak was real and that the compound was a monohydrate. This was fully verified, first, by the completed structural analysis and subsequently by chemical analysis, as has been explained previously. The coordinates assigned on the basis of the second $\rho_z(x,y)$ map are given in table 2, column 2. Two successive $\rho_z(x,y)$ maps were then prepared, the second of which contained 152 F_{hk0}'s, on an absolute scale, corresponding to all of the non-zero intensities measured. Parameters derived from this last map were then used in fixing the signs of the $F_{hk\ell}$'s entering in a bounded electron density projection described below.

All of the atoms are well resolved in the electron density projection $\rho_z(x,y)$ except V and O_{III}. To obtain parameters for these atoms and to check the parameters of the other atoms, the projection on (001) of the electron density between z = 0 and z = $\frac{1}{2}$ was prepared,

following the method of Booth (1948). The expression for the bounded projection of interest here has the form

$$(1)\quad S(x,y)) = \frac{1}{2}\left[\frac{1}{A}\sum_{h}^{\infty}\sum_{k}^{\infty} F_{hk0}\cos 2\pi(hx+ky) - \frac{2\pi}{A}\sum_{h}\sum_{k}^{\infty}\sum_{\ell=-\infty}^{\ell=2n+1}\frac{F_{hk\ell}}{\ell}\sin 2\pi(hx+ky)\right]$$

The first sum within the brackets of equation 1 is simply the usual electron density projection on (001); hence the equation may be rewritten as

$$(2)\quad S(x,y) = \frac{1}{2}\left[\rho_z(x,y) - \frac{2}{\pi A}S'(x,y)\right]$$

where

$$(3)\quad S'(x,y) = \sum_{h}\sum_{k}^{\infty}\sum_{\ell=-\infty}^{\ell=2n+1}\frac{F_{hk\ell}}{\ell}\sin 2\pi(hx+ky)$$

For the space group Pnam equation (3) reduces to

$$(4)\quad \frac{S'(x,y)}{4} = \sum_{h}\sum_{k}^{h+k=2n}{}'_{0} F'_{hk}\sin 2\pi hx\cos 2\pi ky + \sum_{h}\sum_{k}^{h+k=2n+1}{}'_{0} F'_{hk}\cos 2\pi hx\sin 2\pi ky$$

where

$$F'_{hk} = \sum_{\ell=-\infty}^{\infty}{}'_{0}\frac{F_{hk\ell}}{\ell}$$

In evaluating S'(x,y) the $F_{hk\ell}$ values for $\ell \neq 1$ ($\ell = 2n + 1$), were derived from the F_{hk1} values in the following way: it was assumed that within a sufficient degree of approximation the shapes of the scattering curves of the atoms involved are the same as that of some average reference atom. In the present case the reference scattering curve was taken as the average of those of K^+ and V, because these atoms contribute much more to the scattering than do the O atoms. If one writes the atomic scattering factor in the form

$$f_i\,(hk\ell) = Z_i\; g(hk\ell)$$

where $g(hk\ell)$ defines the shape of the reference scattering curve, then for Pnam and $z = \frac{1}{4}$ for the atoms of the asymmetric unit, it follows that

$$\frac{F_{hk1}}{g(hk1)} = -\frac{F_{hk3}}{g(hk3)} = \frac{F_{hk5}}{g(hk5)} = \cdots\cdots\cdots = (-1)^{\frac{n-1}{2}} \left[\frac{F_{hkn}}{g(hkn)}\right]$$

The function S'(x,y) was evaluated with the magnitudes of the $F_{hk\ell}$'s on an arbitrary scale, the signs being calculated from the atomic parameters obtained from the last $\rho_z(x,y)$ map. The scale of S'(x,y) was adjusted to make the average electron density of the bounded projection zero in regions where the heavy atoms do not appear in this projection. The parameters derived from this first bounded projection are given in column 3 of table 2.

The bounded projection used here involves the difference of two separate series, the first a cosine series having as coefficients the F_{hk0} values and the second a sine series with the $(F_{hk\ell})/\ell$ values as coefficients. Distortion is introduced into the bounded projection if two series of unequal length are used, i.e., if the cosine and sine series are not terminated at the same value of $(\sin\theta)/\lambda$. A second source of

distortion will arise if the experimental threshold values of the observed $F_{hk\ell}$ values are different for the (hk0) and (hkl) zones. If these threshold values are appreciably different, an imbalance in the number of terms of small magnitude in each of the two series results.

With these facts in mind, a second bounded projection was evaluated. The $F_{hk\ell}$ values were put in on an absolute basis and no $F_{hk\ell}$ term for which $(\sin\theta)/\lambda > 0.7\ A^{-1}$ was used. For each $F_{hk\ell}$ observed to be absent, for reflections up to and including $(\sin\theta)/\lambda = 0.7\ A^{-1}$, the experimentally determined threshold value was substituted. This second bounded projection, shown in figure 3a, is relatively free from distortion and considerably improved in this respect over the first one. The $\rho_z(x,y)$ map used in the preparation of this bounded projection is shown in figure 3b.

Finally, a least-squares analysis of the x and y parameters of O_I, O_{II}, and O_{III} was carried out using unweighted coefficients, and based on the parameters of column 3, table 2. The final parameters are given in column 4, table 2. For O_I, O_{II}, and O_{III} these were obtained by applying the least-squares corrections. For the K, V, and H_2O parameters, the data of all of the electron density projections were considered to arrive at the best choice. The standard errors associated with the oxygen atom parameters obtained from the least-squares analysis are very nearly the same for the three atoms; the averages are $\varepsilon_x = 0.016$ A and $\varepsilon_y = 0.018$ A. It was assumed that the limiting error in the V and K parameters was that of fixing the peak positions from the electron density maps. Assuming this to be a maximum of 0.001 in cycles, the corresponding standard errors are $\varepsilon_x = 0.004$ A and $\varepsilon_y = 0.007$ A. The

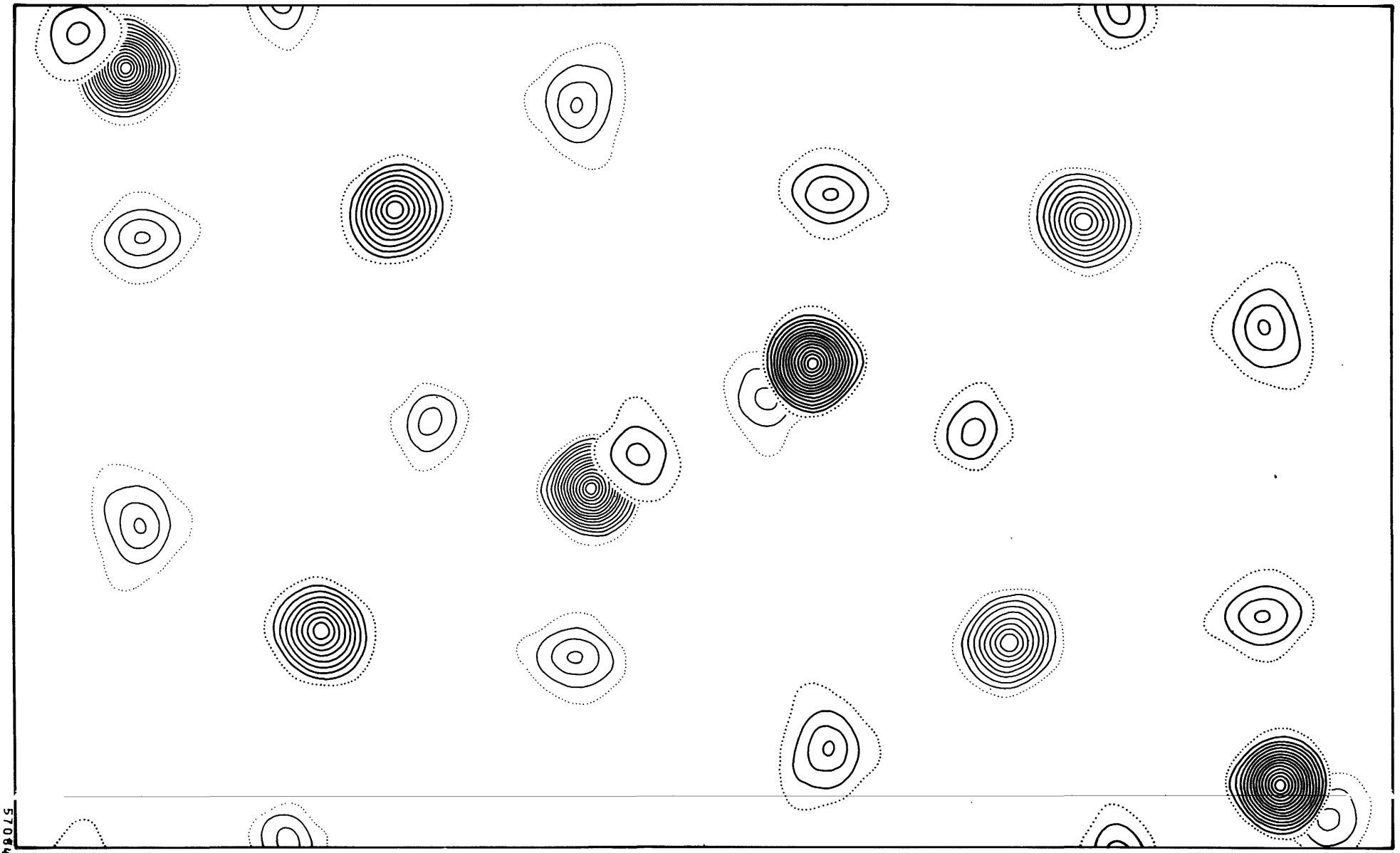

Figure 3a.--Projection on (001) of the superimposed electron density maps taken between z = 0 and z = $\frac{1}{2}$ and between z = $\frac{1}{2}$ and z = 1 for $KVO_3 \cdot H_2O$ (a axis vertical, b horizontal). Contoured at intervals of 4 e. A^{-2}, with the dotted contour equal to 4 e. A^{-2}.

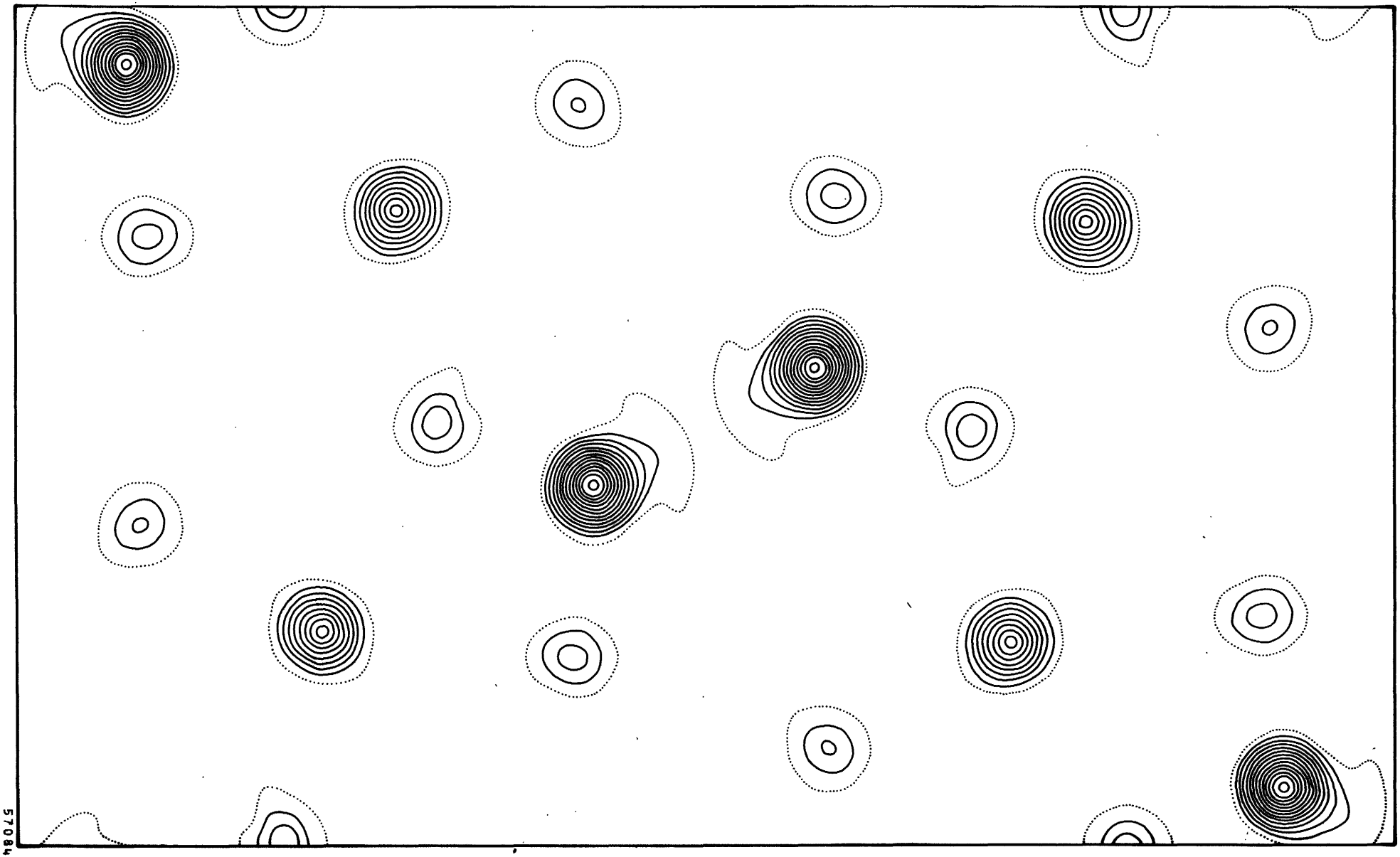

Figure 3b.--Electron density projection $\rho_z(x,y)$ for $KVO_3 \cdot H_2O$ (a axis vertical, b horizontal). Contoured in the same way as figure 3a.

above errors lead to standard errors in the bond lengths of approximately ± 0.02 A for V-O and K-O bonds, and ± 0.03 A for O-O bonds. The corresponding error in O-V-O bond angles is about ± 1°. The precise positioning of the H_2O molecule was not considered to be of any real importance; the standard errors of its x and y parameters are of the order of 0.03 A.

Throughout the course of the structure analysis plots of R' vs sin θ, as suggested by Luzzati (1952), were found to be very helpful in deciding whether the structure was converging. Such a plot based upon the final parameters and compared with the corresponding theoretical curves of Luzzati indicates a maximum mean error in bond length, $|\overline{\Delta r}| = 0.04$ A, entirely in agreement with the least-squares results.

DESCRIPTION AND DISCUSSION OF THE STRUCTURE

A pictorial view of the structure of $KVO_3 \cdot H_2O$ is given in figure 5, and a projected view in figure 4a. It is seen that each vanadium atom is linked to five oxygen atoms to form a distorted trigonal dipyramid. The trigonal dipyramidal polyhedra share edges to form continuous chains parallel to the c axis, accounting for the observed pronounced fibrous cleavage. The coordination of oxygen atoms around the vanadium atoms is shown in detail in figure 6; the corresponding vanadium-oxygen bond lengths and angles and others of importance in the structure are listed in table 3. As shown in the projected view of figure 4a, O_I, O_{II}, and O_{III} lie at the vertices of a triangle containing the vanadium atom, which is displaced away from the center of the triangle toward the edge $O_I O_{II}$. The vanadium-oxygen bonds lying in the triangle are: $V - O_I = 1.63$, $V - O_{II} = 1.67$, $V - O_{III} = 1.99$ A. The plane defined

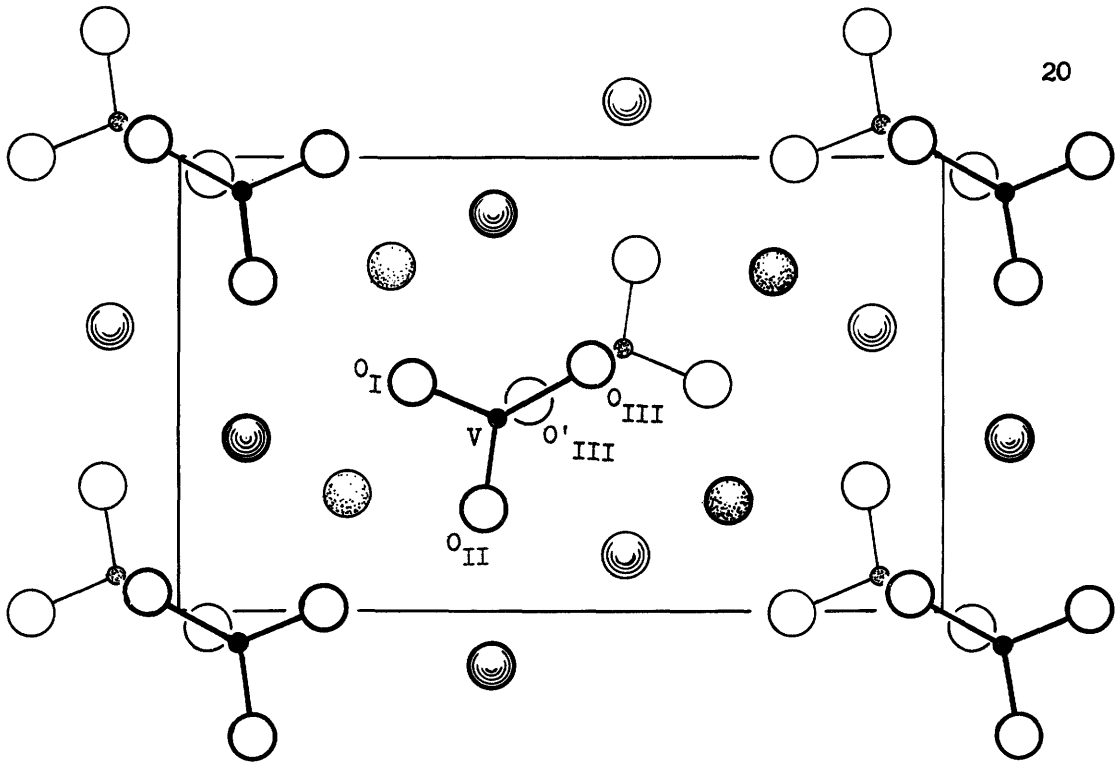

Figure 4a.--Structure of $KVO_3 \cdot H_2O$ projected on (001).

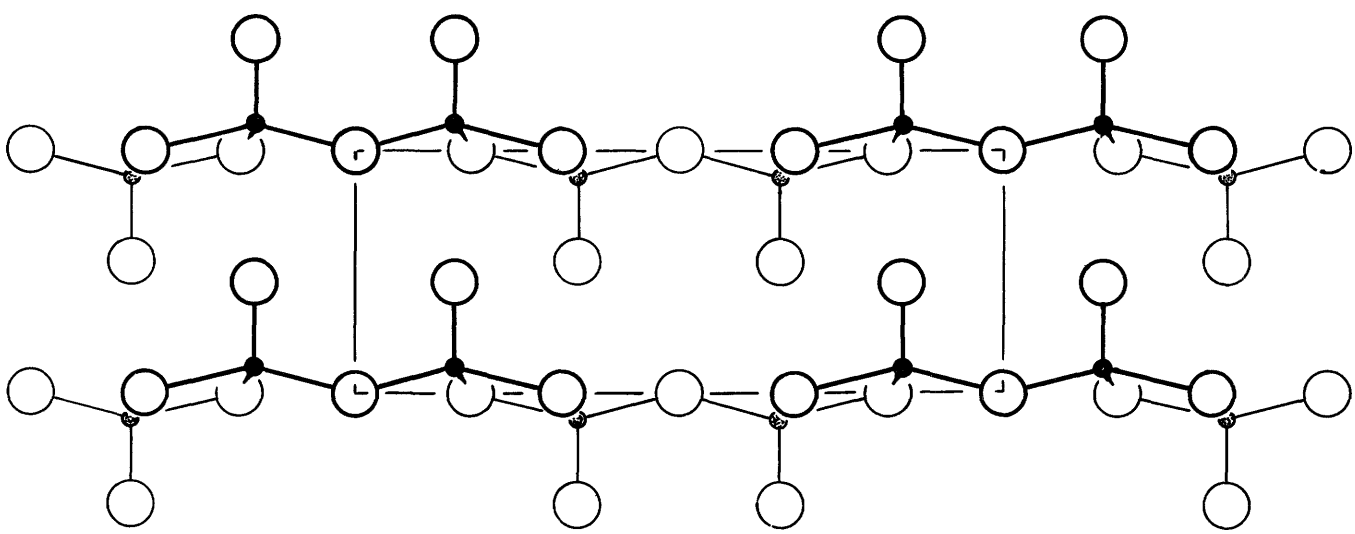

Figure 4b.--Structure of V_2O_5 projected on (001), after Byström et al. (1950).

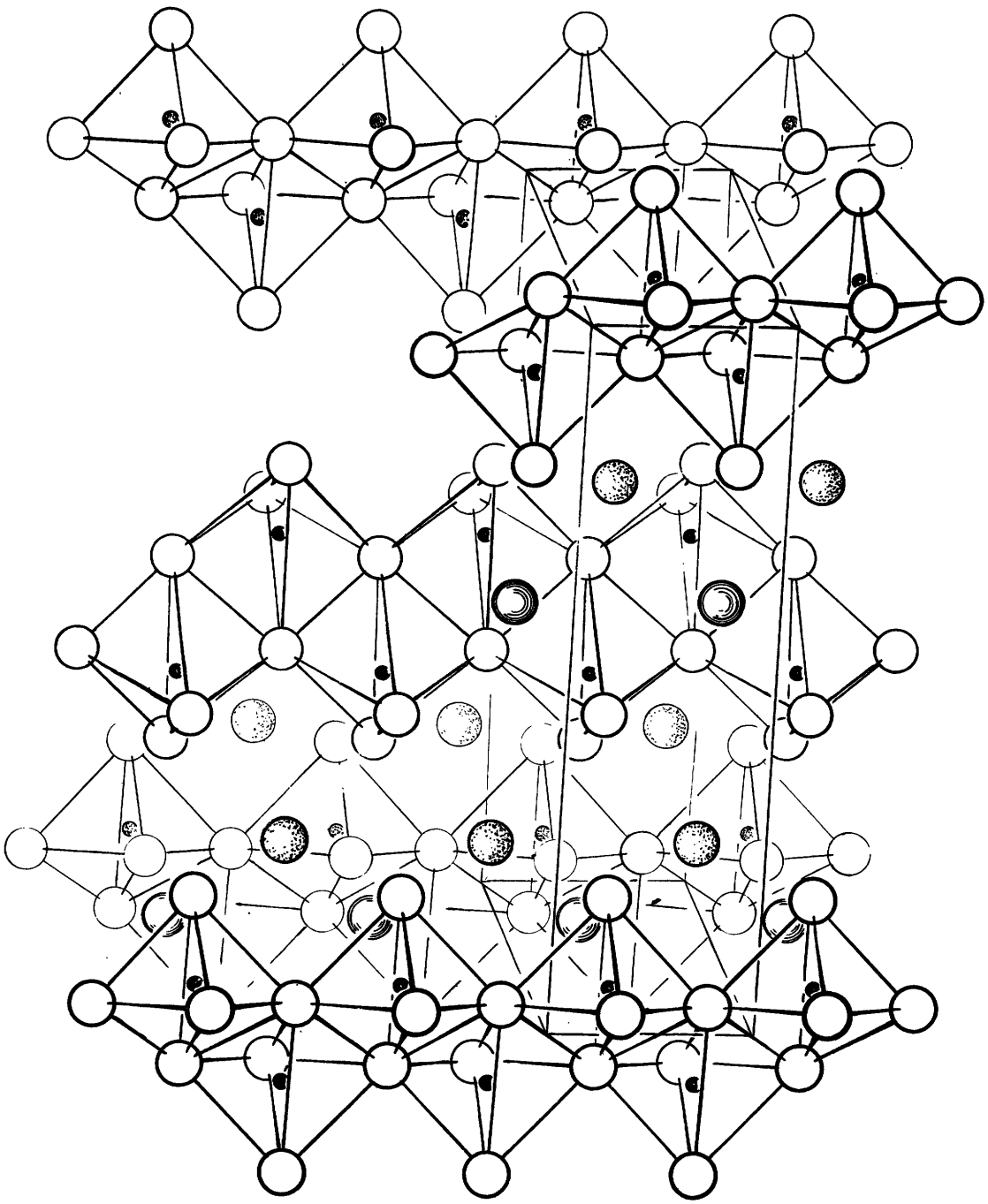

Figure 5.—Pictorial view of $KVO_3 \cdot H_2O$

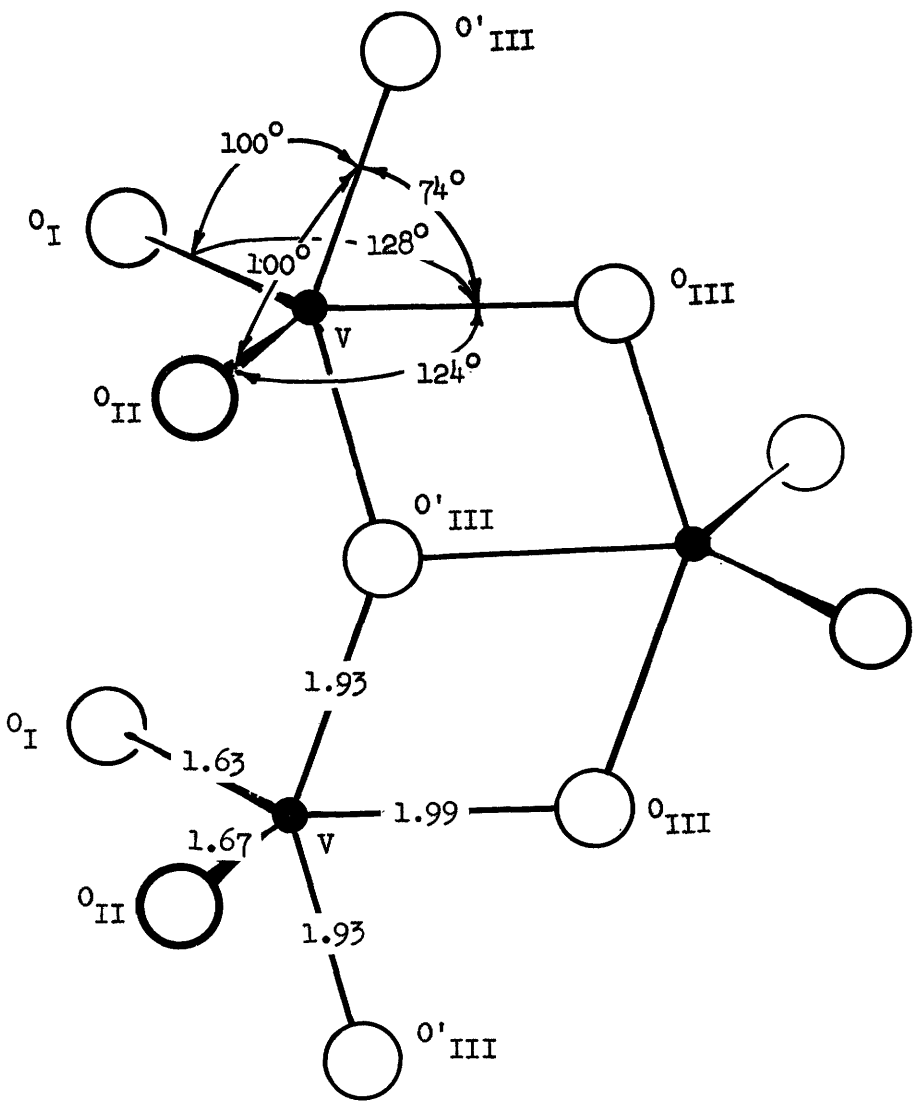

Figure 6.--Details of vanadium-oxygen coordination for $KVO_3 \cdot H_2O$.

as that plane containing the vanadium atoms and parallel to the c axis, also contains the O_{III} atoms. If the bond lengths V - O_I and V - O_{II}, and the bond angles O_I - V - O_{III} and O_{II} - V - O_{III} were the same, respectively, this plane would then be a plane of symmetry. The lengths V - O_I and V - O_{II} were found to be 1.63 $\pm$ 0.02 and 1.67 $\pm$ 0.02 A, respectively. A rough statistical calculation shows that there is high probability that the V - O_{II} bond is truly longer than the V - O_I bond. This conclusion is supported by the difference in bond angles found. It seems probable therefore that the chain does not conform exactly to a plane of symmetry. Detailed examination of the structure shows that the O_I - K and O_{II} - K lengths are different: K - O_I is 2.79 $\pm$ 0.02 A, and K - O_{II} is 3.10 $\pm$ 0.02 A. Thus, it seems likely that the small departures from planar symmetry in the chain are due to packing effects which result in overall lowering of the lattice energy. The O_{III} - O_{III} distance of 2.34 A is quite short and results from strong polarization of these atoms by the vanadium atoms. This postulated polarization is in agreement with the experimental observation that the atomic scattering curve for neutral vanadium gave better results than did that for V^{+5}.

Fivefold coordination in crystals is rare. The only analogous situation seems to be that of V_2O_5 (Byström et al., 1950). In this compound there is a quite similar distorted trigonal dipyramidal polyhedral chain linkage as may be seen by comparing figs. 4a and 4b. The chains as found for $KVO_3 \cdot H_2O$ are further linked in V_2O_5 through oxygen atoms to form the more condensed system. The bond lengths of interest in the two compounds are compared in table 4. For what has here been designated the V - O_I bond, the length in V_2O_5 (1.77A) is significantly

longer than that in $KVO_3 \cdot H_2O$ (1.63 A). This is to be expected because in V_2O_5 it is this oxygen atom which links the chains together to form sheets. The bond in V_2O_5 corresponding to the $V - O_{II}$ bond of $KVO_3 \cdot H_2O$ is quite short, being only 1.54 A in length, and must therefore be quite highly polarized. The differences in the configurations of the chains of the two compounds are such that despite the much smaller V - O bond length in V_2O_5 the smallest O - O separations are nearly the same for the two compounds. The other bonds common to the two compounds have very nearly the same lengths. It is interesting that V_2O_5 is yellow red whereas $KVO_3 \cdot H_2O$ is colorless. It is difficult to decide what differences in the bonding of the two compounds leads to this difference of absorption in the visible spectrum. It is to be hoped that the results of crystal structure analysis of other vanadates being carried out in this and other laboratories will permit this question to be dealt with effectively later.

The K^+ of $KVO_3 \cdot H_2O$ is surrounded by six oxygen atoms and two water molecules in roughly cubic coordination with the K - O bond lengths given in table 3.

Comparisons of the observed and calculated structure factors for the zones (hk0) and (hkl) are listed in tables 5 and 6.

ACKNOWLEDGMENTS

We are indebted to two colleagues of the U. S. Geological Survey: Richard F. Marvin who furnished material for chemical analysis and George B. Magin, Jr., who made the analysis. This work was completed as part of a program undertaken by the U. S. Geological Survey on behalf of the Division of Raw Materials of the Atomic Energy Commission.

Table 1.--X-ray powder data for $KVO_3 \cdot H_2O$ and KVO_3

These data correspond to a mixture of $KVO_3 \cdot H_2O$ and KVO_3 which is obtained when crystals of $KVO_3 \cdot H_2O$ are powdered. The $d_{hk\ell}$ values for $KVO_3 \cdot H_2O$ are calculated from the lattice constants given in the text; the $d_{hk\ell}$ values for KVO_3 are derived from the following data: orthorhombic a = 5.70, b = 10.82, c = 5.22 A. The lines were indexed with the help of a KVO_3 powder pattern. Cu/Ni radiation λ = 1.5418 A was used. Data listed only for $d_{hk\ell} > 2.00$ A. The lines corresponding to KVO_3 are so indicated, the other lines being due to $KVO_3 \cdot H_2O$.

Measured		Calculated		
I	$d_{hk\ell}$	$d_{hk\ell}$	hkℓ	
15	7.00	6.99	110	
5	5.39	5.41	020	KVO_3
9	5.20	5.22 5.22	001 120	KVO_3
10	3.910	3.904 3.924	210 120	 KVO_3
8	3.748	3.756	021	KVO_3
10	3.488	3.495	220	
7	3.262	3.268	111	
14	3.128	3.135 3.136	140 121	 KVO_3
11	3.024	3.017 3.030	121 230	
13	2.854	2.850 2.864	200 031	KVO_3
4	2.735	2.738	201	
11	2.680	2.684 2.702	211 131	
8	2.607	2.609 2.610	240 002	 KVO_3
7	2.526	2.521 2.523	220 320	KVO_3

Table 1.--Continued

Measured		Calculated		
I	$d_{hk\ell}$	$d_{hk\ell}$	hkℓ	
8	2.440	2.437	211	KVO_3
5	2.402	2.402	041	KVO_3
7	2.342	2.343	231	
7	2.302	2.318	112	KVO_3
9	2.257	2.261 2.264	250 060	
4	2.179	2.182	160	
4	2.125	2.122	340	
3	2.043	2.038	400	

Table 2.--Atomic positional parameters for $KVO_3 \cdot H_2O$

Parameters: 2/		Stage of refinement 1/				
		1	2	3	4 (final)	
V	x	0.07	0.073	0.074	0.074	
	y	0.08	0.080	0.082	0.082	
K	x	-0.23	-0.244	-0.244	-0.244	
	y	-0.28	-0.279	-0.278	-0.278	
O_I	x		-0.003	-0.005	-0.005	
	y		0.198	0.195	0.192	
O_{II}	x		0.267	0.276	0.277	
	y		0.100	0.095	0.096	
O_{III}	x		-0.058	-0.046	-0.041	
	y		-0.042	-0.048	-0.047	
H_2O	x		0.125	0.119	0.118	
	y		0.420	0.414	0.412	
R 3/		0.45	0.316	0.159	0.142	(hk0)
				0.194	not calc.	(hkl)

1/ See text for description of stage of refinement.
2/ All atoms in the asymmetric unit at $z = \frac{1}{4}$.
3/ Discrepancy factor.

Table 3.--Bond lengths and bond angles for $KVO_3 \cdot H_2O$

Bond lengths (A)		Bond angles (°)	
V - O_I	1.63	O_I - V - O_{II}	106
V - O_{II}	1.67	O_I - V - O_{III}	128
V - O'_{III}	1.93 (2)	O_{II} - V - O_{III}	124
V - O_{III}	1.99	O'_{III} - V - O'_{III}	147
(V-O bonds ± 0.02)		O_I - V - O'_{III}	100
		O_{II} - V - O'_{III}	100
O_I - O_{II}	2.64	(all ± 1)	
O_I - O'_{III}	2.73		
O_{II} - O'_{III}	2.75		
O_{III} - O'_{III}	2.34 (2)		
(O-O bonds ± 0.03)			
K - O_I	2.98 (2), 2.79 (2)		
K - O_{II}	3.10 (2)		
K - H_2O	2.79 (2)		
(K-O bonds ± 0.02; K-H_2O bonds ± 0.04)			
V - V	3.14 ± 0.02		

Table 4.--Comparison of bond lengths for $KVO_3 \cdot H_2O$ and V_2O_5

	$KVO_3 \cdot H_2O$	V_2O_5
$V - O_I$	1.63 A	1.77 ± 0.03 A
$V - O_{II}$	1.67	1.54 ± 0.06
$V - O'_{III}$	1.93	1.88 ± 0.04
$V - O_{III}$	1.99	2.02 ± 0.08
$O_I - O_{II}$	2.64	2.63
$O_I - O'_{III}$	2.73	2.70
$O_{II} - O'_{III}$	2.75	2.73
$O_{III} - O'_{III}$	2.34	2.39

Table 5.--Observed and calculated structure factors, hk0
Values of F_c based on the atomic coordinates of column 4, table 2

hk0	F_o	F_c	hk0	F_o	F_c
000		304	250	47.4	-43.9
200	15.4	13.5	260		8.1
400	55.8	51.3	270	20.5	18.9
600	63.7	-69.1	280	46.6	-43.2
800	6.1	7.8	290	43.3	38.5
10,0,0	7.2	-14.1	2,10,0		- 3.7
12,0,0	16.6	17.9	2,11,0	21.0	19.2
			2,12,0	22.3	21.6
020	10.2	9.8	2,13,0	9.0	- 9.5
040	16.6	-12.0	2,14,0		- 8.3
060	105.2	-111.6	2,15,0	25.3	-22.8
080	55.0	-46.7	2,16,0	10.8	19.0
0,10,0	39.9	39.7	2,17,0	8.2	- 7.8
0,12,0	28.9	22.3	2,18,0	20.5	-26.0
0,14,0	25.9	26.2	2,19,0		6.5
0,16,0	20.7	-29.8	2,20,0		6.5
0,18,0	17.7	- 9.5	2,21,0	14.1	13.3
0,20,0	8.4	-12.7	2,22,0		- 3.4
0,22,0		18.1			
			310	56.8	55.6
110	56.6	82.5	320	42.8	-45.6
120	21.0	-22.3	330	18.7	-14.5
130	3.6	- 2.2	340	15.9	-11.6
140	73.0	-73.8	350		- 4.5
150	13.1	- 8.0	360	53.0	-53.7
160	41.2	41.7	370	35.6	-31.3
170	53.2	-46.9	380	44.3	45.2
180	15.6	-18.2	390		0.3
190	24.8	-19.5	3,10,0	6.1	- 3.7
1,10,0	40.2	45.6	3,11,0	12.5	10.2
1,11,0	22.5	18.8	3,12,0	29.4	33.0
1,12,0	17.7	-24.8	3,13,0		- 0.4
1,13,0	16.4	10.5	3,14,0	21.8	-22.4
1,14,0		3.7	3,15,0		- 1.3
1,15,0	13.3	8.1	3,16,0	16.9	-10.0
1,16,0	14.1	-11.1	3,17,0		- 5.6
1,17,0	14.3	-10.2	3,18,0	8.2	- 4.5
1,18,0		1.6	3,19,0		- 2.6
1,19,0	16.1	-12.0	3,20,0		3.6
1,20,0		8.9	3,21,0		5.8
1,21,0		1.9	3,22,0	17.4	16.4
1,22,0		- 3.5			
			410	33.3	-29.8
210	48.4	-46.4	420	56.3	-56.5
220	69.6	69.0	430	72.2	-79.9
230	75.0	-78.7	440	36.6	41.9
240	39.2	-33.5	450	39.7	-34.7

Table 5.--Continued

hk0	F_o	F_c	hk0	F_o	F_c
460		4.1	6,11,0		5.4
470	22.5	16.7	6,12,0	22.8	-17.9
480		2.2	6,13,0		9.7
490	35.8	36.2	6,14,0	20.7	-23.9
4,10,0		3.9	6,15,0		- 1.5
4,11,0	25.1	18.9	6,16,0	18.2	23.7
4,12,0	24.1	-27.7	6,17,0		1.0
4,13,0	14.6	-13.6	6,18,0		0.6
4,14,0		4.2	6,19,0		- 3.7
4,15,0	20.5	-17.3	6,20,0	16.1	15.0
4,16,0		- 8.3			
4,17,0	9.0	- 7.7	710	25.6	-25.5
4,18,0	9.0	17.3	720	6.7	-12.4
4,19,0		10.2	730	12.5	-13.5
4,20,0		- 2.4	740	8.2	8.4
4,21,0	15.6	10.4	750	33.0	35.6
			760	19.2	-25.7
510	23.8	-20.1	770	18.7	17.7
520	41.0	-36.4	780	14.6	16.8
530	5.1	- 4.7	790		10.4
540	65.5	-73.4	7,10,0	14.8	-19.5
550	30.0	29.6	7,11,0	16.6	-16.6
560	21.8	22.1	7,12,0	10.2	16.0
570	21.5	20.1	7,13,0	23.0	-19.5
580		- 2.1	7,14,0		- 6.7
590		- 8.1	7,15,0		- 3.4
5,10,0	37.9	46.4	7,16,0		6.8
5,11,0	12.0	- 8.8	7,17,0	13.3	10.4
5,12,0	9.5	-16.7	7,18,0		3.0
5,13,0	22.0	-21.7	7,19,0	16.1	10.8
5,14,0	7.2	- 4.5			
5,15,0		3.7	810	11.5	12.8
5,16,0	16.1	-13.8	820	29.2	-38.5
5,17,0	9.0	7.5	830		1.7
5,18,0		3.5	840	20.2	23.3
5,19,0	9.2	5.2	850		7.0
5,20,0	11.5	13.2	860	11.3	10.3
5,21,0		4.6	870		- 8.0
			880	11.5	10.0
610		- 5.3	890	15.9	-13.9
620		0.1	8,10,0		5.1
630		1.4	8,11,0		- 5.4
640		0.1	8,12,0	17.7	-18.6
650	12.3	-16.2	8,13,0		0.7
660	50.9	57.5	8,14,0		0.8
670	7.2	- 8.5	8,15,0	14.3	13.0
680	7.7	6.3	8,16,0		- 5.6
690		- 3.5	8,17,0		6.3
6,10,0	11.5	-14.5	8,18,0	14.6	12.7

Table 5.--Continued

hk0	F_o	F_c	hk0	F_o	F_c
910	18.7	-22.9	11,1,0	11.8	9.0
920	20.7	26.1	11,2,0	14.3	12.3
930		- 2.0	11,3,0		- 8.7
940	7.2	3.9	11,4,0	20.7	22.0
950	18.2	18.9	11,5,0		- 2.9
960	12.0	12.9	11,6,0		- 9.5
970	16.6	19.6	11,7,0	14.1	-12.6
980	24.1	-34.1	11,8,0		- 3.8
990	7.7	- 6.1	11,9,0		8.4
9,10,0		- 3.4	11,10,0	19.7	-23.3
9,11,0	8.2	- 4.6	11,11,0		8.2
9,12,0	7.7	- 9.6	11,12,0		7.7
9,13,0	9.0	-13.3	11,13,0		6.7
9,14,0	15.9	18.4			
9,15,0		7.0	12,1,0		8.5
9,16,0	10.0	9.6	12,2,0		-10.4
9,17,0		7.2	12,3,0		0.4
			12,4,0		4.3
10,1,0	7.2	5.7	12,5,0	8.4	6.7
10,2,0	8.2	8.6	12,6,0		- 9.4
10,3,0	22.3	24.4	12,7,0		- 1.5
10,4,0	8.2	-13.1	12,8,0		- 3.9
10,5,0	8.2	3.8	12,9,0		- 5.9
10,6,0	8.2	8.9	12,10,0		7.2
10,7,0	8.2	- 8.6	12,11,0		- 2.7
10,8,0		- 3.0			
10,9,0	15.6	-18.5	13,1,0	9.5	8.7
10,10,0		4.2	13,2,0		7.5
10,11,0		- 7.9	13,3,0		- 1.0
10,12,0		7.1	13,4,0		- 2.8
10,13,0		9.6	13,5,0		-11.2
10,14,0		- 7.1	13,6,0		7.7
10,15,0		8.0	13,7,0		- 6.8
			13,8,0		-10.1

Table 6.--Observed and calculated structure factors, hkl
Values of F_c based on the atomic coordinates of column 3, table 2

hkl	F_o	F_c	hkl	F_o	F_c
201	48.6	-51.8	211	58.9	-77.2
401	55.1	-52.6	221	33.5	-29.2
601	21.6	20.4	231	46.4	46.1
801	17.3	12.7	241	35.6	33.3
10,0,1	33.5	35.2	251	27.0	-27.8
12,0,1	9.2	2.8	261	49.7	49.2
14,0,1		7.1	271	15.7	12.8
16,0,1	11.9	-14.8	281	20.0	21.3
			291	33.5	35.4
011	*	-24.5	2,10,1	18.4	-18.8
031	105.8	-132.4	2,11,1		- 2.0
051	14.0	6.8	2,12,1	36.2	-38.3
071	36.7	32.3	2,13,1		15.3
091	75.6	78.2	2,14,1	18.4	-19.4
0,11,1	23.2	29.9	2,15,1	25.4	-36.6
0,13,1	33.5	-45.3	2,16,1	8.1	7.3
0,15,1	23.2	-19.6	2,17,1	8.6	- 3.2
0,17,1	28.1	-43.2	2,18,1	18.9	23.4
0,19,1	19.4	29.4	2,19,1		-13.2
0,21,1	16.2	7.9	2,20,1	13.5	14.1
0,23,1	14.6	16.0	2,21,1	15.7	18.4
			2,22,1		- 2.0
111	30.8	-37.1	2,23,1		5.4
121	35.6	-36.4	2,24,1	13.0	-12.2
131	34.0	34.4			
141	10.8	4.5	311	8.6	- 1.6
151	7.0	- 8.5	321	31.3	-31.0
161	9.2	- 6.9	331	29.2	-23.3
171	50.2	56.4	341	7.0	- 0.2
181	39.4	37.5	351	53.5	53.1
191	34.0	-41.4	361	8.6	2.7
1,10,1	36.2	31.6	371		-12.7
1,11,1		9.6	381	23.2	23.3
1,12,1		- 1.5	391	30.8	37.5
1,13,1	25.9	-31.3	3,10,1	14.6	18.5
1,14,1	17.8	-15.0	3,11,1	38.3	-46.6
1,15,1		10.0	3,12,1	14.0	-12.3
1,16,1	27.5	-28.8	3,13,1	18.4	-12.3
1,17,1	8.1	7.8	3,14,1	7.6	- 6.7
1,18,1	8.6	- 9.9	3,15,1	16.7	-19.8
1,19,1	9.2	1.5	3,16,1	8.1	-13.8
1,20,1	13.0	9.6	3,17,1	17.8	11.6
1,21,1		9.2	3,18,1		- 0.4
1,22,1	12.4	10.7	3,19,1	20.0	25.2
1,23,1		-12.5	3,20,1	9.7	8.1

Table 6.--Continued

hkl	F_o	F_c
3,25,1	18.4	-26.7
411	35.6	36.5
421	23.2	-16.1
431		- 6.3
441	31.9	29.4
451	43.2	40.8
461	48.1	51.3
471	17.8	-17.7
481	21.6	15.7
491		- 5.2
4,10,1	30.8	-25.4
4,11,1	11.9	- 4.6
4,12,1	32.4	-38.4
4,13,1	9.2	-15.1
4,14,1	21.6	-21.3
4,15,1	20.5	28.0
4,16,1	14.6	13.3
4,17,1		-15.3
4,18,1	20.5	20.3
4,19,1	9.2	15.6
4,20,1	11.9	15.7
4,24,1	10.8	- 9.5
511	41.6	-38.2
521	23.8	16.7
531	24.3	25.1
541	42.7	39.9
551	23.2	14.3
561	9.7	-11.6
571	48.1	58.4
581	15.7	-11.5
591	30.2	-35.1
5,10,1	25.4	-19.9
5,11,1	15.7	-10.1
5,12,1	14.0	- 3.7
5,13,1	31.3	-42.5
5,14,1	16.7	15.0
5,15,1	8.6	6.8
5,16,1	8.6	8.2
5,17,1	16.2	16.6
5,18,1		1.8
5,19,1	14.6	12.4
611	14.6	-19.1
621		- 0.1
631	62.6	75.9
641		4.3
651	13.0	3.2
661		- 3.6
671	20.0	-17.1
681		- 0.4
691	30.2	-26.9
6,10,1		0.7
6,11,1	28.6	-30.7
6,12,1	13.5	- 9.8
6,13,1	19.4	27.3
6,14,1		- 6.3
6,15,1	18.4	9.8
6,16,1		- 6.2
6,17,1	18.4	23.3
6,18,1		6.7
6,19,1		-14.8
6,20,1		8.0
6,21,1	12.4	- 6.8
711	15.7	11.9
721	28.1	23.6
731	11.9	-12.1
741	34.0	30.6
751	18.4	24.0
761	5.9	1.5
771	25.9	-26.9
781	27.5	-27.1
791	11.9	17.8
7,10,1	24.8	-20.9
7,11,1	16.7	-23.2
7,12,1	14.6	-14.2
7,13,1	7.6	6.9
7,14,1	19.4	23.4
7,15,1		- 6.5
7,16,1	22.7	19.0
7,21,1	13.0	- 2.9
811	24.3	26.9
821	15.1	16.2
831	6.5	- 1.0
841	6.5	- 6.3
851	23.8	23.3
861	14.0	- 9.3
871	18.9	-19.0
881	15.7	-14.6
891	17.3	-14.0
8,10,1	7.0	- 2.9
8,11,1	15.1	- 7.6
8,12,1	16.2	8.8

Table 6.--Continued

hkl	F_o	F_c
8,13,1		- 6.5
8,14,1		4.3
8,15,1	23.8	29.5
8,21,1	10.8	-19.7
911	24.3	22.8
921	17.3	15.3
931	10.8	12.5
941	24.8	27.0
951	28.6	-34.8
961	15.1	-15.8
971	14.0	- 5.5
981	16.7	-16.1
991	20.5	-22.4
9,10,1	17.3	-20.3
9,11,1	23.8	28.5
9,12,1		3.9
9,13,1	9.2	3.9
9,14,1	18.9	18.8
9,15,1	9.7	8.8
9,16,1		12.0
9,17,1	10.3	-10.5
9,18,1		0.7
9,19,1	13.0	-13.7
10,1,1	16.7	-24.3
10,2,1	14.6	7.1
10,3,1	14.6	15.2
10,4,1	11.3	- 7.0
10,5,1	11.3	-13.9
10,6,1	23.2	-25.4
10,7,1		- 2.2
10,8,1	17.8	-12.7
10,9,1		2.6
10,10,1	14.0	10.3
10,11,1		- 9.5
10,12,1	17.3	13.0
10,13,1		12.1
10,14,1	13.5	11.1
10,15,1		- 5.2
10,16,1	8.6	- 7.9
10,17,1		11.4
10,18,1	10.8	- 7.8
11,1,1	25.9	24.6
11,2,1	12.4	-14.9
11,3,1	7.6	- 8.8
11,4,1	13.5	-14.4
11,5,1	10.8	- 5.6
11,6,1		- 1.5
11,7,1	29.7	-34.8
11,8,1	8.1	4.0
11,9,1	9.7	11.4
11,10,1	8.6	12.9
11,11,1		4.6
11,12,1		- 6.8
11,13,1	20.5	23.3
12,1,1		5.1
12,2,1		7.9
12,3,1	19.4	-21.4
12,4,1		- 6.5
12,5,1		- 0.7
12,6,1	9.2	- 4.5
12,7,1		- 7.5
12,8,1		- 7.7
12,9,1	12.4	8.5
12,10,1		1.2
12,11,1		8.9
12,12,1	12.4	9.3
13,1,1		1.6
13,2,1	17.3	-19.5
13,3,1		3.5
13,4,1	9.2	-10.8
13,5,1	9.2	-12.9
13,6,1	9.2	-12.2
13,7,1		6.1
13,8,1	13.5	15.4
13,9,1		- 8.2
13,10,1		5.9
13,11,1	13.0	15.2
14,1,1	14.6	-21.1
14,2,1		- 6.5
14,3,1		- 6.1
14,4,1		0.3
14,5,1	9.2	-15.1
14,6,1		- 4.0
14,7,1		5.1
14,8,1		1.3
14,9,1	10.8	15.0
15,1,1	9.2	-11.3
15,2,1	9.2	-10.8
15,3,1		- 7.1
15,4,1	10.8	-11.1
15,5,1	13.0	18.3
15,6,1		0.3

*Not registered.

REFERENCES

Booth, A. D. (1948). Fourier Technique in X-ray Organic Structure Analysis. Cambridge: University Press.

Buerger, M. J. (1951). Acta Cryst. 4, 531.

Buerger, M. J., and Klein, G. E. (1945). J. Appl. Phys. 16, 416.

Byström, A, Wilhelmi K.-A., and Brotzen, O. (1950). Acta Chem. Scand. 4, 1119.

Christ, C. L., Clark, Joan R., and Evans, H. T. Jr. (1953). J. Chem. Phys. 21, 1114.

Cochran, W. (1948). J. Sci. Instr. 25, 253.

Ducret, L.-P. (1951). Ann. de Chemie (12th series) 6, 705.

Dullberg, P. (1903). Z phys. Chem. 45, 129.

Fock, A. (1889). Z. Krystallogr. 17, 1.

International Tables for the Determination of Crystal Structures (1935). Berlin: Borntraeger.

Jander, G., and Jahr, K. F. (1933). Z. anorg. Chem. 212, 1.

Luzzati, V. (1952). Acta Cryst. 5, 802.

Norblad, J.-A. (1875). Bull.Soc. Chim. (2nd series) 23, 64.

Souchay, P., and Carpeni, G. (1946). Bull. Soc. Chim. (5th series) 13, 160.